

Slow-roll Inflation with the Gauss-Bonnet and Chern-Simons Corrections

Masaki Satoh*

*Department of Physics, Kyoto University, Kyoto 606-8501, Japan

(Dated: October 30, 2018)

We study slow-roll inflation with the Gauss-Bonnet and Chern-Simons corrections. We obtain general formulas for the observables: spectral indices, tensor-to-scalar ratio and circular polarization of gravitational waves. The Gauss-Bonnet term violates the consistency relation $r = -8n_T$. Particularly, blue spectrum $n_T > 0$ and scale invariant spectrum $|8n_T|/r \ll 1$ of tensor modes are possible. These cases require the Gauss-Bonnet coupling function of $\xi_{,\phi} \sim 10^8/M_{\text{Pl}}$. We use examples to show new-inflation-type potential with $10M_{\text{Pl}}$ symmetry breaking scale and potential with flat region in $\phi \gtrsim 10M_{\text{Pl}}$ lead to observationally consistent blue and scale invariant spectra, respectively. Hence, these interesting cases can actually be realized. The Chern-Simons term produce circularly polarized tensor modes. We show an observation of these signals supports existence of the Chern-Simons coupling function of $\omega_{,\phi} \sim 10^8/M_{\text{Pl}}$. Thus, with future observations, we can fix or constrain the value of these coupling functions, at the CMB scale.

PACS numbers:

I. INTRODUCTION

Currently, the concept of slow-roll inflation is widely accepted by cosmologists, due to many precise observations, such as the Wilkinson Microwave Anisotropy Probe (WMAP)[1]. We can explain all observations simply, using single field slow-roll inflation. However, future observations might detect non-standard signals, which will be evidence for a non-standard inflationary theory. The energy scale of inflation is considered to be very high compared to current experimental scale. Thus, we can say that a new inflationary theory might contain information with regard to high energy physics, such as a superstring theory. Therefore it is important to study theories beyond standard single field slow-roll inflation.

One of candidates for a modified inflationary model is inflation with the Gauss-Bonnet and Chern-Simons corrections. These are the only two meaningful combinations of second order curvature terms, as a low energy effective theory[34], and can also be derived from some superstring models[2]. Cosmology with the Gauss-Bonnet term can affect background evolution and result in a non-singular cosmological model[2–15] or other interesting solutions[16–25]. In inflation with the Chern-Simons term, primordial gravitational waves are circularly polarized[26–30], which is considered as an interesting target for some future observations[31–33]. Many authors studied Gauss-Bonnet and Chern-Simons modified inflation. However, *slow-roll* inflation with the Gauss-Bonnet terms is not much studied, except in the papers[35, 36]. Taking current observations into consideration, slow-roll inflation is the most plausible paradigm for inflation. Therefore investigating slow-roll inflation with the Gauss-Bonnet and Chern-Simons corrections is an important subject.

We have studied this topic in the previous paper[35]. In this paper, we re-formalize slow-roll inflation in gravity with the Gauss-Bonnet and Chern-Simons corrections. We derive formulas for the observables, namely the scalar spectral index n_S , the tensor spectral index n_T , the tensor-to-scalar ratio r and the circular polarization ratio Π , in our inflationary model. The Gauss-Bonnet term violates the consistency relation $r = -8n_T$. We show if this violation is observationally confirmed, the derivative of the Gauss-Bonnet coupling function at the observation scale, namely the Cosmic Microwave Background (CMB) scale, is fixed. We study the two typical cases, blue and scale invariant spectra of tensor modes. Because blue and scale invariant mean $n_T > 0$ and $|8n_T|/r \ll 1$, respectively, these cases strongly violate this consistency relation. If these are confirmed in future observations, the Gauss-Bonnet coupling function must be $\xi_{,\phi} \sim 10^8/M_{\text{Pl}}$, at the CMB scale. Of course, even if no such effects are observed in future, we can get the constraint $\xi_{,\phi} \lesssim 10^8/M_{\text{Pl}}$, at least. However, it is unclear whether these interesting cases are consistent with current observations. Therefore, we perform calculations in some concrete examples. We show new-inflation-type potential with symmetry breaking scale of $10M_{\text{Pl}}$ leads to an observationally consistent blue spectrum; potential with flat region in $\phi \gtrsim 10M_{\text{Pl}}$ leads to a consistent scale invariant spectrum. In both cases, the almost constant $\xi_{,\phi}$ is required. The Chern-Simons term leads to circular polarization of gravitational waves. We show if this circular

*Electronic address: satoht@tap.scphys.kyoto-u.ac.jp

polarization is detected, we can fix the derivative of the Chern-Simons coupling function, at the CMB scale. It might be $\omega_{,\phi} \sim 10^8/M_{\text{Pl}}$. Therefore, the value of the Gauss-Bonnet and Chern-Simons coupling functions at the CMB scale will be fixed, or constrained, with future observations.

We organize this paper as follows: In section II, the action we considered is shown and slow-roll inflation in this action is studied, calculations of perturbations in slow-roll inflation is in section III, interesting features of our model are mentioned in section IV, and section V is for conclusion.

II. SLOW-ROLL INFLATION

We consider the following action:

$$S = \int d^4x \sqrt{-g} \left[\frac{M_{\text{Pl}}^2}{2} R - \frac{1}{2} \nabla_\alpha \phi \nabla^\alpha \phi - V(\phi) \right] - \frac{1}{16} \int d^4x \sqrt{-g} \xi(\phi) R_{\text{GB}}^2 + \frac{1}{16} \int d^4x \sqrt{-g} \omega(\phi) R \tilde{R} , \quad (1)$$

where $M_{\text{Pl}}^2 \equiv 1/8\pi G$ is the reduced Planck mass, R_{GB}^2 and $R \tilde{R}$ are the Gauss-Bonnet and Chern-Simons combinations. These combinations are defined by

$$R_{\text{GB}}^2 \equiv R_{\alpha\beta\gamma\delta} R^{\alpha\beta\gamma\delta} - 4R_{\alpha\beta} R^{\alpha\beta} + R^2 \quad (2)$$

$$R \tilde{R} \equiv \frac{1}{2} \epsilon^{\alpha\beta\gamma\delta} R_{\alpha\beta\rho\sigma} R_{\gamma\delta}{}^{\rho\sigma} , \quad (3)$$

where $\epsilon^{\alpha\beta\gamma\delta}$ is the Levi-Civita anti-symmetric tensor. Hence, the Chern-Simons correction represents parity violation in gravity. This action is composed of the Einstein-Hilbert term and a canonical scalar field which couples to the Gauss-Bonnet and Chern-Simons terms through the coupling functions $\xi(\phi)$ and $\omega(\phi)$. Note that only these two types of higher curvature corrections, namely the Gauss-Bonnet and Chern-Simons terms, are essential as a low energy effective theory[34]. Here, we take these terms as small corrections. In principle, coupling functions must be fixed by quantum gravity, such as a superstring theory. However, it is impossible to determine these coupling functions, because we haven't succeeded to construct quantum gravity. Therefore, we treat these as free functions and attempt to fix or constrain these coupling functions from cosmological observations. Through these attempts, we may get new information with regard to quantum gravity, because these coupling functions are related to properties of quantum gravity.

Here, as a background metric, we choose the flat Friedmann-Robertson-Walker(FRW) metric:

$$d^2s = -dt^2 + a^2(t) \delta_{ij} dx^i dx^j , \quad (4)$$

where $a(t)$ denotes a scale factor which describes cosmic expansion. Varying Eq.(1) in the FRW metric, Eq.(4), we get background equations:

$$3M_{\text{Pl}}^2 H^2 = \frac{1}{2} \dot{\phi}^2 + V + \frac{3}{2} H^3 \dot{\xi} \quad (5)$$

$$\ddot{\phi} + 3H\dot{\phi} + \frac{3}{2} H^2 (\dot{H} + H^2) \xi_{,\phi} + V_{,\phi} = 0 , \quad (6)$$

where a dot denotes a time derivative and the Hubble parameter H is defined by $H \equiv \dot{a}/a$. Because of parity symmetry of Eq.(4), the Chern-Simons correction cannot affect these background equations. We take $\dot{\phi} < 0$ throughout this paper.

Here we focus on the case in which scalar field is slowly rolling and its friction term is dominating Eq.(6). In other words, we take slow-roll approximations:

$$\frac{\dot{\phi}^2}{M_{\text{Pl}}^2 H^2} \ll 1 , \quad \frac{\ddot{\phi}}{H\dot{\phi}} \ll 1 . \quad (7)$$

In this paper, we consider the Gauss-Bonnet term as a *small* correction. Hence, it must be much smaller than the Einstein-Hilbert term, energetically speaking. The following inequality, hence, must be satisfied:

$$\frac{H^3 \dot{\xi}}{2M_{\text{Pl}}^2 H^2} = \frac{H\dot{\xi}}{2M_{\text{Pl}}^2} \ll 1 . \quad (8)$$

Under Eqs.(7) and (8), the background equation, Eq.(5), become

$$H^2 = \frac{V}{3M_{\text{Pl}}^2} . \quad (9)$$

This equation doesn't contain the Gauss-Bonnet correction since it is energetically negligible, of course. The time derivative of the Hubble parameter becomes

$$\frac{\dot{H}}{H^2} = \frac{(\dot{H}^2)}{2H^3} = \frac{V_{,\phi}\dot{\phi}}{6M_{\text{Pl}}^2 H^3} = \frac{1}{2} \frac{V_{,\phi}}{V} \frac{\dot{\phi}}{H} . \quad (10)$$

The another background equation, Eq.(6), is

$$\dot{\phi} = -\frac{V_{,\phi}}{3H} - \frac{1}{2} H^3 \xi_{,\phi} - \frac{1}{2} H \dot{H} \xi_{,\phi} . \quad (11)$$

The last term in the right-hand side can be written as

$$-\frac{1}{2} H \dot{H} \xi_{,\phi} = -\frac{1}{4} \frac{V_{,\phi}}{V} H^2 \dot{\xi} = -\frac{V_{,\phi}}{3H} \frac{H \dot{\xi}}{4M_{\text{Pl}}^2} . \quad (12)$$

Hence, this term is negligible compared with the first term in the right-hand side of Eq.(8), and Eq.(6) becomes

$$\frac{\dot{\phi}}{M_{\text{Pl}} H} = -M_{\text{Pl}} \frac{V_{,\phi}}{V} - \frac{V \xi_{,\phi}}{6M_{\text{Pl}}^3} . \quad (13)$$

This equation shows that the Gauss-Bonnet coupling function ξ works as effective potential. In our inflationary model, slow-roll equations are Eq.(9) and (13). We can see only the equation of motion, Eq.(13), is modified. Here, we define the new function ζ :

$$\zeta(\phi) \equiv V_{,\phi} + \frac{V^2 \xi_{,\phi}}{6M_{\text{Pl}}^4} . \quad (14)$$

Eq.(13) becomes

$$\frac{\dot{\phi}}{M_{\text{Pl}} H} = -\frac{M_{\text{Pl}}}{V} \zeta . \quad (15)$$

In our model, the expression for the e-folding number N is written as

$$N = \int dt H = \int_{\phi}^0 d\phi \frac{H}{\dot{\phi}} = \frac{1}{M_{\text{Pl}}^2} \int_0^{\phi} d\phi \frac{V}{\zeta} = \frac{1}{M_{\text{Pl}}^2} \int_0^{\phi} d\phi \frac{1}{V_{,\phi}/V + V \xi_{,\phi}/6M_{\text{Pl}}^4} , \quad (16)$$

where we assume that potential has a minimum at $\phi = 0$.

We must consider consistency conditions for Eqs.(9) and (15). First, we check slow-roll conditions, Eqs.(7):

$$\frac{\dot{\phi}^2}{M_{\text{Pl}}^2 H^2} = M_{\text{Pl}}^2 \frac{\zeta^2}{V^2} \ll 1 , \quad (17)$$

$$\frac{\ddot{\phi}}{H\dot{\phi}} = \frac{1}{\dot{\phi}} \frac{d\dot{\phi}}{dt} + \frac{\dot{H}}{H^2} = -M_{\text{Pl}}^2 \frac{d\zeta}{d\phi} \frac{1}{V} - \frac{M_{\text{Pl}}^2}{2} \frac{\zeta V_{,\phi}}{V^2} = \frac{M_{\text{Pl}}^2}{2} \frac{\zeta V_{,\phi}}{V^2} - M_{\text{Pl}}^2 \frac{\zeta_{,\phi}}{V} \ll 1 . \quad (18)$$

Second, the condition for smallness of the Gauss-Bonnet term, Eq.(8), is

$$\frac{H \dot{\xi}}{2M_{\text{Pl}}^2} = \frac{H \dot{\phi}}{2M_{\text{Pl}}^2} \xi_{,\phi} = -\frac{1}{2} \frac{H^2}{V} \zeta \xi_{,\phi} = -\frac{1}{6M_{\text{Pl}}^2} \zeta \frac{6M_{\text{Pl}}^4}{V^2} (\zeta - V_{,\phi}) = M_{\text{Pl}}^2 \frac{\zeta V_{,\phi}}{V^2} - M_{\text{Pl}}^2 \frac{\zeta^2}{V^2} \ll 1 . \quad (19)$$

Here, we define three slow-roll parameters:

$$\alpha \equiv \frac{M_{\text{Pl}}^2}{2} \frac{\zeta V_{,\phi}}{V^2} , \quad \beta \equiv \frac{M_{\text{Pl}}^2}{2} \frac{\zeta^2}{V^2} , \quad \gamma \equiv M_{\text{Pl}}^2 \frac{\zeta_{,\phi}}{V} . \quad (20)$$

It is clear that if $|\alpha|, \beta, |\gamma| \ll 1$ are realized, all consistency conditions are satisfied and slow-roll inflation occurs. In the case of conventional slow-roll inflation, $\zeta = V_{,\phi}$ is realized. Hence, α and β becomes conventional ϵ , and γ becomes η . For later convenience, we derive expressions for \dot{H}/H^2 , $\dot{\phi}$ and $H\dot{\xi}/M_{\text{Pl}}^2$ in slow-roll parameters. From Eqs.(10), (15) and (19), we get

$$\frac{\dot{H}}{H^2} = -\frac{1}{2} \frac{V_{,\phi}}{V} \frac{M_{\text{Pl}}^2}{V} \zeta = -\frac{M_{\text{Pl}}^2}{2} \frac{\zeta V_{,\phi}}{V^2} = -\alpha, \quad \frac{\dot{\phi}}{M_{\text{Pl}} H} = -\sqrt{2\beta}, \quad \frac{H\dot{\xi}}{M_{\text{Pl}}^2} = 4(\alpha - \beta). \quad (21)$$

Remember that we are taking $\dot{\phi} < 0$. As in a conventional scenario, the time derivative of the Hubble parameter is small. In the case that α can be treated as a constant, we can solve the equation for H easily:

$$H = \frac{1}{\alpha t}, \quad a = a_0 |t|^{1/\alpha}, \quad (22)$$

where a_0 is a constant of integration. Because we choose $H > 0$, $t > 0$ for $\alpha > 0$ and $t < 0$ for $\alpha < 0$.

The most important difference between our model and a conventional inflation is that, in our model super inflation can be realized, while in a conventional one it cannot. In our model, the slow-roll parameter α can take a negative value. From Eqs.(21), we can see this leads to super inflation, $\dot{H} > 0$. We can expect that if this super inflation phase corresponds to the CMB scale, an observationally interesting signal could be detected in future experiments, and this signal might be regarded as evidence for existence of gravitational higher curvature terms.

Here, we show an interesting effect of the Gauss-Bonnet correction in slow-roll inflation. Let us consider general potential $V(\phi)$, which does not satisfies conventional slow-roll conditions. If we set

$$\xi(\phi) = \frac{6M_{\text{Pl}}^4}{V(\phi)}, \quad (23)$$

$\zeta(\phi) = 0$ is realized. This makes all slow-roll parameters zero, and inflation occurs. This shows that, even if we use extremely steep potential, slow-roll inflation can be achieved due to the Gauss-Bonnet correction.

III. PERTURBATIONS

In this section, we perform perturbative calculations on the background of slow-roll inflation. First, we study scalar and tensor modes of perturbations. Note that no vector modes plays an important role since there is no source for vectors. Second, we derive expressions for reconstructing the value of potential and coupling functions using observables. Finally, we briefly comment on the Lyth bound in our model.

A. Scalar perturbations

Here, we consider scalar perturbations in the flat FRW background. The metric is

$$ds^2 = a^2(\tau) [-(1 + 2A)d\tau^2 + B_{|i}d\tau dx^i + (\delta_{ij} + 2\psi\delta_{ij} + 2E_{|ij})dx^i dx^j], \quad (24)$$

where τ is the conformal time $d\tau \equiv dt/a$ and a bar denotes a spacial derivative. Latin indices run from 1 to 3. In the case of slow-roll inflation, τ becomes

$$\tau = \frac{1}{a_0} \frac{1}{1 - 1/\alpha} t |t|^{-1/\alpha} = \frac{t}{1 - 1/\alpha} \frac{1}{a} = -\frac{1}{1 - \alpha} \frac{1}{aH}, \quad (25)$$

where $\tau < 0$. We fix gauge as $E = \delta\phi = 0$, where $\delta\phi$ is a perturbation of scalar field ϕ . This gauge is useful in this case, because the perturbative quantity ψ can be treated as a master variable and $-\psi$ coincide with the gauge invariant comoving curvature perturbation \mathcal{R} . Of course, this is a complete choice of gauge. Here, we concentrate on ψ , because what we need is the power spectrum of ψ in super-horizon scale. Expanding ψ in Fourier modes,

$$\psi = \frac{1}{M_{\text{Pl}}} \int \frac{dk^3}{(2\pi)^3} \psi_{\mathbf{k}} e^{i\mathbf{k}\cdot\mathbf{x}}, \quad (26)$$

the action for ψ becomes

$$S = \frac{1}{2} \int d\tau \int \frac{dk^3}{(2\pi)^3} A_\psi^2 (|\psi'_{\mathbf{k}}|^2 - C_\psi^2 k^2 |\psi_{\mathbf{k}}|^2), \quad (27)$$

where a prime denotes a conformal time derivative and

$$A_\psi^2 \equiv a^2 \left(\frac{1 - \sigma/2}{1 - 3\sigma/4} \right)^2 \left(\frac{\dot{\phi}^2}{M_{\text{Pl}}^2 H^2} + \frac{3}{8} \frac{\sigma^2}{1 - \sigma/2} \right), \quad (28)$$

$$C_\psi^2 \equiv 1 + \frac{a^2}{A_\psi^2} \left(\frac{\sigma}{1 - 3\sigma/4} \right)^2 \left[-\frac{\sigma}{16} + \frac{\ddot{\xi}}{16M_{\text{Pl}}^2} + \frac{\dot{H}}{2H^2} \left(1 - \frac{\sigma}{2} \right) \right], \quad (29)$$

and σ is defined by

$$\sigma \equiv \frac{H\dot{\xi}}{M_{\text{Pl}}^2}. \quad (30)$$

This action contains only ξ . This is because scalar perturbations in the flat FRW background have parity symmetry. Let us define the new variable $\Psi_{\mathbf{k}}$, by $\Psi_{\mathbf{k}} \equiv A_\psi \psi_{\mathbf{k}}$, and the above action becomes

$$S = \frac{1}{2} \int d\tau \int \frac{d\mathbf{k}^3}{(2\pi)^3} \left(|\Psi'_{\mathbf{k}}|^2 - C_\psi^2 k^2 |\Psi_{\mathbf{k}}|^2 + \frac{A''_\psi}{A_\psi} |\Psi_{\mathbf{k}}|^2 \right). \quad (31)$$

This leads to the equation of motion:

$$\Psi''_{\mathbf{k}} + \left(C_\psi^2 k^2 - \frac{A''_\psi}{A_\psi} \right) \Psi_{\mathbf{k}} = 0. \quad (32)$$

Here, we impose slow-roll approximation, and derive the expressions for A_ψ^2 and C_ψ^2 up to first order in slow-roll parameters. Remember that the time derivative of the Hubble parameter H is first order. In computing primordial power spectra, we treat slow-roll parameters as constants of time. We get the following equations:

$$\sigma = 4(\alpha - \beta), \quad \frac{\dot{\phi}^2}{M_{\text{Pl}}^2 H^2} = 2\beta, \quad \frac{\ddot{\xi}}{M_{\text{Pl}}^2} = \frac{\dot{\sigma}}{H} - \frac{\dot{H}}{H^2} \sigma = 0, \quad (33)$$

and

$$A_\psi^2 = a^2 (1 + \sigma/2) 2\beta = 2a^2 \beta, \quad C_\psi^2 = 1. \quad (34)$$

Let us consider the effective potential A''_ψ/A_ψ . For this purpose, we derive some equations:

$$\frac{\dot{\beta}}{H\beta} = \frac{2\dot{\zeta}}{H\zeta} - \frac{2\dot{V}}{HV} = \frac{2\zeta_{,\phi}\dot{\phi}}{\zeta H} - \frac{2V_{,\phi}\dot{\phi}}{V H} = -2M_{\text{Pl}}^2 \frac{\zeta_{,\phi}}{V} + 2M_{\text{Pl}}^2 \frac{\zeta V_{,\phi}}{V^2} = 4\alpha - 2\gamma, \quad (35)$$

$$\frac{A'_\psi}{A_\psi} = \frac{a(A_\psi^2)'}{2A_\psi^2} = aH + \frac{a\dot{\beta}}{2\beta} = aH(1 + 2\alpha - \gamma) = \frac{1}{-\tau} \frac{1 + 2\alpha - \gamma}{1 - \alpha} = \frac{1 + 3\alpha - \gamma}{-\tau}. \quad (36)$$

Hence

$$\frac{A''_\psi}{A_\psi} = \frac{d}{d\tau} \left(\frac{A'_\psi}{A_\psi} \right) + \left(\frac{A'_\psi}{A_\psi} \right)^2 = \frac{1 + 3\alpha - \gamma}{\tau^2} + \frac{1 + 6\alpha - 2\gamma}{\tau^2} = \frac{2 + 9\alpha - 3\gamma}{\tau^2} = \frac{\nu_\psi^2 - 1/4}{\tau^2}, \quad (37)$$

where ν_ψ is defined by

$$\nu_\psi \equiv \frac{3}{2} + 3\alpha - \gamma. \quad (38)$$

Eq.(32) becomes

$$\Psi''_{\mathbf{k}} + \left(k^2 - \frac{\nu_\psi^2 - 1/4}{\tau^2} \right) \Psi_{\mathbf{k}} = 0. \quad (39)$$

To quantize the quantity Ψ , we replace Ψ with the operator $\hat{\Psi}$ and expand this as

$$\hat{\Psi}_{\mathbf{k}} = v_{\mathbf{k}}(\tau) \hat{a}_{\mathbf{k}} + v_{-\mathbf{k}}^*(\tau) \hat{a}_{-\mathbf{k}}^\dagger, \quad (40)$$

where $\hat{a}_{\mathbf{k}}$ and $\hat{a}_{-\mathbf{k}}^\dagger$ are annihilation and creation operators. The mode function $v_{\mathbf{k}}(\tau)$ obeys the same equation as $\Psi_{\mathbf{k}}$ does, namely Eq.(39):

$$v_{\mathbf{k}}'' + \left(k^2 - \frac{\nu_\psi^2 - 1/4}{\tau^2} \right) v_{\mathbf{k}} = 0 . \quad (41)$$

For solving this equation, we must impose an initial condition. Because effective potential vanishes in asymptotic past, we can choose the Bunch-Davies vacuum at $\tau \rightarrow -\infty$:

$$v_{\mathbf{k}} = \frac{1}{\sqrt{2k}} e^{-ik\tau} . \quad (42)$$

Under this condition, Eq.(41) has the analytic solution

$$v_{\mathbf{k}}(\tau) = \frac{\sqrt{-\pi\tau}}{2} e^{i(\pi/4 + \pi\nu_\psi/2)} H_{\nu_\psi}^{(1)}(-k\tau) , \quad (43)$$

where $H_{\nu_\psi}^{(1)}$ is the first kind of Hankel function.

Here, we derive the expression for the power spectrum of scalar perturbation \mathcal{P}_S in super-horizon, which is defined by

$$\langle 0 | \hat{\psi}^\dagger \hat{\psi} | 0 \rangle = \int d(\log k) \frac{1}{M_{\text{Pl}}^2} \frac{1}{2\pi^2} k^3 \frac{|v_{\mathbf{k}}|^2}{A_\psi^2} = \int d(\log k) \mathcal{P}_S(k) . \quad (44)$$

In super-horizon, $-k\tau \ll 1$, $v_{\mathbf{k}}(\tau)$ has the asymptotic form

$$v_{\mathbf{k}}(\tau) = \sqrt{\frac{-\tau}{2(-k\tau)^3}} e^{i(-\pi/4 + \pi\nu_\psi/2)} \frac{\Gamma(\nu_\psi)}{\Gamma(3/2)} \left(\frac{-k\tau}{2} \right)^{3/2 - \nu_\psi} . \quad (45)$$

Hence \mathcal{P}_S becomes

$$\mathcal{P}_S(k) = \frac{1}{M_{\text{Pl}}^2} \frac{1}{4\pi^2} \frac{1}{A_\psi^2 \tau^2} \left(\frac{\Gamma(\nu_\psi)}{\Gamma(3/2)} \right)^2 \left(\frac{-k\tau}{2} \right)^{3 - 2\nu_\psi} = \frac{1}{8\pi^2 \beta} \left(\frac{H}{M_{\text{Pl}}} \right)^2 \left(\frac{-k\tau}{2} \right)^{3 - 2\nu_\psi} . \quad (46)$$

The scalar power spectrum is of order $H^2/(\beta M_{\text{Pl}}^2)$, and this is easily understood because $\mathcal{P}_S \sim (H^2/\dot{\phi})^2 \sim H^2/(\beta M_{\text{Pl}}^2)$, in which we use Eq.(21). The scalar spectral index n_S becomes

$$n_S - 1 = 3 - 2\nu_\psi = -6\alpha + 2\gamma . \quad (47)$$

If we take $\xi = 0$, the slow-roll parameters α and γ coincide with the conventional ones ϵ and η , respectively. Hence, in this case, the expression for n_S takes ordinary form.

B. Tensor perturbations

In this subsection, we compute perturbations of tensor modes. The metric is

$$ds^2 = a^2(\tau) [-d\tau^2 + (\delta_{ij} + h_{ij}) dx^i dx^j] , \quad (48)$$

where h_{ij} denotes a transverse-traceless tensor on a constant-time hypersurface. Hence it satisfies $h_i^i = h_{ij|j} = 0$. We expand h_{ij} , which is gauge-invariant because tensor modes have no gauge freedom, in Fourier modes and circular polarization:

$$h_{ij} = \frac{\sqrt{2}}{M_{\text{Pl}}} \sum_{\pm} \int \frac{dk^3}{(2\pi)^3} \phi_{\mathbf{k}}^{\pm} e^{i\mathbf{k}\cdot\mathbf{x}} p_{\mathbf{k},ij}^{\pm} , \quad (49)$$

where $p_{\mathbf{k},ij}^{\pm}$ is the polarization tensor for circular polarization and \pm denotes the helicity of each polarization mode. Note that $\sqrt{2}$ and M_{Pl} are for later convenience. The action for $\phi_{\mathbf{k}}^{\pm}$ becomes

$$S = \sum_{\pm} \frac{1}{2} \int d\tau \frac{dk^3}{(2\pi)^3} A_{\text{T}}^2 (|(\phi_{\mathbf{k}}^{\pm})'|^2 - C_{\text{T}}^2 |\phi_{\mathbf{k}}^{\pm}|^2) , \quad (50)$$

where

$$A_{\text{T}}^2 \equiv a^2 \left(1 - \frac{\sigma}{2} \mp \frac{1}{M_c} \frac{k}{a} \Omega \right), \quad C_{\text{T}}^2 \equiv 1 + \frac{a^2}{A_{\text{T}}^2} \frac{\sigma}{2} - \frac{\ddot{\xi}}{2M_{\text{Pl}}^2} \frac{a^2}{A_{\text{T}}^2}. \quad (51)$$

The mass scale M_c corresponds to the UV cut-off scale of our model and Ω is defined by

$$\Omega \equiv \frac{1}{2} \frac{M_c}{M_{\text{Pl}}} \frac{\dot{\omega}}{M_{\text{Pl}}}. \quad (52)$$

Note that we omit \pm symbols in the expressions for A_{T}^2 and C_{T}^2 for simplicity. The Chern-Simons coupling function ω doesn't appear in the background and scalar perturbations, but, at the same time, this appears in tensor perturbations, because *circular* modes clearly violate parity symmetry.

From Eqs.(51), we can see that if $|\Omega| > 1$, A_{T}^2 takes a negative value in one of helicity modes at the cut-off scale $k/a = M_c$. This is very important because it implies the appearance of ghost modes in gravitational waves. Since we don't know proper treatment for ghost modes, we impose the condition $|\Omega| < 1$. For simplicity of following calculation, we take Ω as a constant, which is justified in many models because ϕ is slowly rolling. We can always treat the Chern-Simons correction $k\Omega/M_c a$ as a small correction, because $|\Omega| < 1$ and $k/a < M_c$. Of course, $|\Omega| > 1$ model might lead to very drastic results and such model is interesting itself. However, we don't analyze this situation in this paper.

Introducing the new variable $\mu_{\mathbf{k}} \equiv A_{\text{T}} \phi_{\mathbf{k}}^{\pm}$, Eq.(50) can be rewritten as

$$S = \sum_{\pm} \frac{1}{2} \int d\tau \int \frac{d^3k}{(2\pi)^3} \left(|\mu'_{\mathbf{k}}|^2 - C_{\text{T}}^2 k^2 |\mu_{\mathbf{k}}|^2 + \frac{A'_{\text{T}}}{A_{\text{T}}} |\mu_{\mathbf{k}}|^2 \right). \quad (53)$$

Hence the equation of motion for $\mu_{\mathbf{k}}$ is

$$\mu''_{\mathbf{k}} + \left(C_{\text{T}}^2 k^2 - \frac{A''_{\text{T}}}{A_{\text{T}}} \right) \mu_{\mathbf{k}} = 0, \quad (54)$$

where we also omit \pm in a $\mu_{\mathbf{k}}$ expression.

Considering slow-roll inflation, we compute spectra up to first order in slow-roll parameters and Ω . The quantities A_{T} and C_{T} become

$$A_{\text{T}}^2 = a^2 \left(1 - 2\alpha + 2\beta \mp \frac{k\Omega}{M_c a} \right), \quad C_{\text{T}}^2 = 1 + 2\alpha - 2\beta, \quad (55)$$

and we get

$$\frac{A'_{\text{T}}}{A_{\text{T}}} = \frac{a}{2} \frac{(A_{\text{T}}^2)'}{A_{\text{T}}^2} = \frac{a}{2} \left(2H \pm \frac{k\Omega}{M_c a} H \right) = aH \pm k \frac{\Omega}{2M_c} H = \frac{1+\alpha}{-\tau} \pm k \frac{H}{2M_c} \Omega. \quad (56)$$

Effective potential becomes

$$\frac{A''_{\text{T}}}{A_{\text{T}}} = \frac{d}{d\tau} \left(\frac{A'_{\text{T}}}{A_{\text{T}}} \right) + \left(\frac{A'_{\text{T}}}{A_{\text{T}}} \right)^2 = \frac{1+\alpha}{\tau^2} + \frac{1+2\alpha}{\tau^2} \pm \frac{k}{-\tau} \frac{H}{M_c} \Omega = \frac{2+3\alpha}{\tau^2} \pm \frac{k}{-\tau} \frac{H}{M_c} \Omega = \frac{\nu_{\text{T}}^2 - 1/4}{\tau^2} \pm \frac{k}{-\tau} \frac{H}{M_c} \Omega, \quad (57)$$

where ν_{T} is defined by

$$\nu_{\text{T}} \equiv \frac{3}{2} + \alpha. \quad (58)$$

Hence, Eq.(54) becomes

$$\mu''_{\mathbf{k}} + \left(C_{\text{T}}^2 k^2 - \frac{\nu_{\text{T}}^2 - 1/4}{\tau^2} \mp \frac{k}{-\tau} \frac{H}{M_c} \Omega \right) \mu_{\mathbf{k}} = 0. \quad (59)$$

Let us quantize perturbations. We promote $\mu_{\mathbf{k}}$ to the operator $\hat{\mu}_{\mathbf{k}}$ and expand in the annihilation and creation operators $\hat{a}_{\mathbf{k}}$ and $\hat{a}_{-\mathbf{k}}^{\dagger}$:

$$\hat{\mu}_{\mathbf{k}} = u_{\mathbf{k}}(\tau) \hat{a}_{\mathbf{k}} + u_{-\mathbf{k}}^*(\tau) \hat{a}_{-\mathbf{k}}^{\dagger}. \quad (60)$$

The equation for $u_{\mathbf{k}}(\tau)$ is the same as that for $\mu_{\mathbf{k}}(\tau)$, Eq.(59):

$$u_{\mathbf{k}}'' + \left(C_{\text{T}}^2 k^2 - \frac{\nu_{\text{T}}^2 - 1/4}{\tau^2} \mp \frac{k}{-\tau} \frac{H}{M_{\text{c}}} \Omega \right) u_{\mathbf{k}} = 0 . \quad (61)$$

As in the case of scalar modes, effective potential vanishes at asymptotic past. Thus we can use the Bunch-Davies vacuum as the initial condition for Eq.(61). We take at $\tau \rightarrow -\infty$:

$$u_{\mathbf{k}} = \frac{1}{\sqrt{2C_{\text{T}}k}} e^{-iC_{\text{T}}k\tau} . \quad (62)$$

Hence, the solution for Eq.(61) is

$$u_{\mathbf{k}} = e^{-iC_{\text{T}}k\tau} (-2C_{\text{T}}k\tau)^{\nu_{\text{T}}} \sqrt{-\tau} e^{-i(\pi/4 + \pi\nu_{\text{T}}/2)} \text{U} \left(\frac{1}{2} + \nu_{\text{T}} \mp \frac{i}{2C_{\text{T}}} \frac{H}{M_{\text{c}}} \Omega, 1 + 2\nu_{\text{T}}, 2iC_{\text{T}}k\tau \right) \exp \left(\pm \frac{\pi}{4C_{\text{T}}} \frac{H}{M_{\text{c}}} \Omega \right) , \quad (63)$$

where U is the confluent hypergeometric function. This solution has the asymptotic form in super-horizon scale:

$$u_{\mathbf{k}}(\tau) = \sqrt{\frac{-\tau}{2(-C_{\text{T}}k\tau)^3}} e^{i(-\pi/4 + \pi\nu_{\text{T}}/2)} \frac{\Gamma(\nu_{\text{T}})}{\Gamma(3/2)} \left(\frac{-C_{\text{T}}k\tau}{2} \right)^{3/2 - \nu_{\text{T}}} \exp \left(\pm \frac{\pi}{4C_{\text{T}}} \frac{H}{M_{\text{c}}} \Omega \right) \quad (64)$$

We define the power spectra for each polarization mode $\mathcal{P}_{\text{T}}^{\pm}$ and the total power spectrum \mathcal{P}_{T} :

$$\langle 0 | \hat{h}_{ij}^{\dagger} \hat{h}^{ij} | 0 \rangle = \sum_{\pm} \int d(\log k) \frac{1}{M_{\text{Pl}}^2} \frac{2}{\pi^2} k^3 \frac{|u_{\mathbf{k}}|^2}{A_{\text{T}}^2} = \sum_{\pm} \int d(\log k) \mathcal{P}_{\text{T}}^{\pm} = \int d(\log k) \mathcal{P}_{\text{T}} . \quad (65)$$

In super-horizon, these $\mathcal{P}_{\text{T}}^{\pm}$ and \mathcal{P}_{T} become

$$\begin{aligned} \mathcal{P}_{\text{T}}^{\pm} &= \frac{1}{M_{\text{Pl}}^2} \frac{1}{C_{\text{T}}^3} \frac{1}{\pi^2} \frac{1}{A_{\text{T}}^2 \tau^2} \left(\frac{\Gamma(\nu_{\text{T}})}{\Gamma(3/2)} \right)^2 \left(\frac{-C_{\text{T}}k\tau}{2} \right)^{3 - 2\nu_{\text{T}}} \exp \left(\pm \frac{\pi}{2C_{\text{T}}} \frac{H}{M_{\text{c}}} \Omega \right) \\ &= \frac{1 - 3\alpha + \beta}{\pi^2} \left(\frac{H}{M_{\text{Pl}}} \right)^2 \left(\frac{-k\tau}{2} \right)^{3 - 2\nu_{\text{T}}} \left(1 \pm \frac{\pi}{2} \frac{H}{M_{\text{c}}} \Omega \right) \end{aligned} \quad (66)$$

$$\mathcal{P}_{\text{T}} = \frac{2}{\pi^2} (1 - 3\alpha + \beta) \left(\frac{H}{M_{\text{Pl}}} \right)^2 \left(\frac{-k\tau}{2} \right)^{3 - 2\nu_{\text{T}}} . \quad (67)$$

The tensor spectral index n_{T} is

$$n_{\text{T}} = 3 - 2\nu_{\text{T}} = -2\alpha . \quad (68)$$

This expression becomes the same as an ordinary one in the $\xi \rightarrow 0$ limit. Remember that in our model, α can take a negative value in which super inflation, $\dot{H} > 0$, is realized. Hence, this expression shows that in super inflation, a blue spectrum for tensor modes, $n_{\text{T}} > 0$, is realized. The detection of this blue signal might be evidence for this inflationary model, because $n_{\text{T}} < 0$ is always satisfied in a conventional model.

We have derived both scalar and tensor spectra. Thus, we can get the observationally important quantity, namely the tensor-to-scalar ratio r :

$$r \equiv \frac{\mathcal{P}_{\text{T}}}{\mathcal{P}_{\text{S}}} = 16\beta . \quad (69)$$

Note that $\beta \rightarrow \epsilon$ in the $\xi \rightarrow 0$ limit. There is the consistency relation $r = -8n_{\text{T}}$ in ordinary single field slow-roll inflation, or $r \leq -8n_{\text{T}}$ in multi-filed one. However, these consistency relation doesn't hold in our case, because α and β are in principle different quantities. The violation of this relation might be an observationally interesting feature of our model. Note that a blue spectrum of tensor modes can also be interpreted as a strong violation of this relation.

The another important feature of our model is a violation of parity symmetry. Eq.(66) shows that the parity violating Chern-Simons correction results in difference between power spectra of each helicity mode. We quantify this difference using the ratio Π which is defined by

$$\Pi \equiv \frac{\mathcal{P}_{\text{T}}^+ - \mathcal{P}_{\text{T}}^-}{\mathcal{P}_{\text{T}}^+ + \mathcal{P}_{\text{T}}^-} = \frac{\pi}{2} \frac{H}{M_{\text{c}}} \Omega . \quad (70)$$

This quantity Π takes naturally a small value, because $\Omega < 1$ and $H < M_c$. However, we can still expect Π is of order a few percent, which is considered to be observable in future experiments[31–33]. Note that we have got no observational constraint on ω and Ω , because these only appear in tensor modes, which we haven't detected.

In a conventional model, the transformation of potential $V \rightarrow \rho V$, where ρ is constant, has no effect on spectral indices, tensor-to-scalar ratio and e-folding number. Hence, an overall factor of potential is fixed by the scalar power spectrum \mathcal{P}_S . In our model, from Eqs.(20) and (16), it is clear that these observables depend on the transformation $V \rightarrow \rho V$. In this case, the transformations which keep α, β, γ and N constants are $V \rightarrow \rho V$ and $\xi \rightarrow \xi/\rho$.

C. Reconstruction of potential and coupling functions

Slow-roll inflation in the Gauss-Bonnet modified gravity violates the consistency relation $r = -8n_T$. However, in the case of standard multi field inflation, this relation also modified as $r \leq -8n_T$. Therefore, the case of over production of gravitational waves, $r > -8n_T$, is important. From Eqs.(68) and (69), we can see over-production is realized if $\beta > \alpha$ is satisfied. Taking a look at the definition of slow-roll parameters and ζ , Eqs.(20) and (14), we can see in the situation that $\xi_{,\phi} > 0$ is realized, gravitational waves will always be overly produced. Thus, we can expect over production in many models.

If the violation of this relation is observationally confirmed, we can reconstruct the value of the derivative of the Gauss-Bonnet coupling function $\xi_{,\phi}$. From Eqs.(20)

$$\frac{\beta}{\alpha} = \frac{\zeta}{V_{,\phi}} = 1 + \frac{V^2 \xi_{,\phi}}{6M_{\text{Pl}}^4 V_{,\phi}} = 1 + \frac{1}{12M_{\text{Pl}}^2} \frac{\zeta \xi_{,\phi}}{\alpha} = 1 + \frac{\sqrt{2}}{12M_{\text{Pl}}^3} \frac{\sqrt{\beta}}{\alpha} V \xi_{,\phi}. \quad (71)$$

The potential V and the slow-roll parameter β are related by the scalar power spectrum \mathcal{P}_S . From Eq.(46)

$$\mathcal{P}_S = \frac{1}{24\pi^2 \beta} \frac{V}{M_{\text{Pl}}^4}. \quad (72)$$

Hence, $\xi_{,\phi}$ is written as

$$\xi_{,\phi} = \frac{12M_{\text{Pl}}^3}{\sqrt{2}\beta} \frac{1}{V} (\beta - \alpha) = \frac{1}{2\sqrt{2}\pi^2 M_{\text{Pl}}} \frac{1}{\mathcal{P}_S} \frac{\beta - \alpha}{\beta^{3/2}} = \frac{\sqrt{2}}{\pi^2 M_{\text{Pl}}} \frac{1}{\sqrt{r} \mathcal{P}_S} \frac{r + 8n_T}{r}. \quad (73)$$

Let us parameterize the violation ratio of consistency relation by using δ :

$$\delta \equiv \frac{r + 8n_T}{r}. \quad (74)$$

The expression for $\xi_{,\phi}$ becomes

$$M_{\text{Pl}} \xi_{,\phi} = \frac{\sqrt{2}}{\pi^2} \frac{\delta}{\sqrt{r} \mathcal{P}_S} = 1.86 \times 10^6 \left(\frac{\mathcal{P}_S}{2.441 \times 10^{-9}} \right)^{-1} \left(\frac{r}{0.1} \right)^{-1/2} \left(\frac{\delta}{0.01} \right). \quad (75)$$

This equation clearly shows that we can get the value of $\xi_{,\phi}$, or constrain $\xi_{,\phi}$ at least, with observing the tensor-to-scalar ratio r and the violation ratio of consistency relation δ . In other words, we can predict this violation ratio of consistency relation by using this equation for each Gauss-Bonnet inflationary model. The expression for the value of potential, at the CMB scale, is the same as usual. From Eq.(72)

$$\frac{V}{M_{\text{Pl}}^4} = \frac{3\pi^2}{2} r \mathcal{P}_S = 3.61 \times 10^{-9} \left(\frac{\mathcal{P}_S}{2.441 \times 10^{-9}} \right) \left(\frac{r}{0.1} \right). \quad (76)$$

However, the derivative of potential $V_{,\phi}$ suffers modification. From the definition of slow-roll parameters, Eq.(20)

$$\begin{aligned} \frac{V_{,\phi}}{M_{\text{Pl}}^3} &= \frac{2}{M_{\text{Pl}}^8} \frac{V}{\zeta} V \alpha = \frac{\sqrt{2}\alpha V}{M_{\text{Pl}}^4 \sqrt{\beta}} = 24\sqrt{2}\pi^2 \alpha \sqrt{\beta} \mathcal{P}_S = -3\sqrt{2}\pi^2 n_T \sqrt{r} \mathcal{P}_S = \frac{3\sqrt{2}\pi^2}{8} r^{3/2} \mathcal{P}_S (1 - \delta) \\ &= 4.04 \times 10^{-10} \left(\frac{\mathcal{P}_S}{2.441 \times 10^{-9}} \right) \left(\frac{r}{0.1} \right)^{3/2} (1 - \delta). \end{aligned} \quad (77)$$

Using Eqs.(75),(76) and (77), we can fix the value of V , $V_{,\phi}$ and $\xi_{,\phi}$ using observables. The expression for the scalar spectral index n_S contains $V_{,\phi\phi}$ and $\xi_{,\phi\phi}$. However, we cannot separate these quantities in our model. Thus, from

these observables, we cannot fix the value of $V_{,\phi\phi}$ and $\xi_{,\phi\phi}$. To this point, we have studied a general case, placing special emphasis on a violation of consistency relation. However, there are other models which also can violate this relation. Particularly, the model which overly produce tensor modes exists[37]. Therefore in the next section, we will investigate a unique phenomenon in our model, namely a blue spectrum of tensor mode.

Next, let us study the Chern-Simons coupling function. Considering future observations, deriving the expression for $\omega_{,\phi}$ by using observable is meaningful. From the definition of Ω , Eq.(52), $\omega_{,\phi}$ is

$$\begin{aligned} M_{\text{Pl}}\omega_{,\phi} &= M_{\text{Pl}}\frac{\dot{\omega}}{\dot{\phi}} = \frac{2M_{\text{Pl}}^3\Omega}{M_c} \frac{-1}{\sqrt{2\beta}M_{\text{Pl}}H} = -\frac{4M_{\text{Pl}}^2}{\pi} \frac{\Pi}{\sqrt{2\beta}H^2} = -\frac{12M_{\text{Pl}}^4}{\pi} \frac{\Pi}{\sqrt{2\beta}V} = -\frac{\sqrt{2}}{4\pi^3} \frac{\Pi}{\beta^{3/2}\mathcal{P}_S} = -\frac{16\sqrt{2}}{\pi^3} \frac{\Pi}{r^{3/2}\mathcal{P}_S} \\ &= -9.45 \times 10^7 \left(\frac{\mathcal{P}_S}{2.441 \times 10^{-9}} \right)^{-1} \left(\frac{r}{0.1} \right)^{-3/2} \left(\frac{\Pi}{0.01} \right). \end{aligned} \quad (78)$$

Thus, we can see that for confirming existence of the Chern-Simons term, it is important to detect circular polarization in tensor modes. We can also use this expression to predict this polarization ratio. Because $|\Pi| \ll 1$ is required by the definition, Eq.(70), we can get the constraint on the value of $\omega_{,\phi}$:

$$|M_{\text{Pl}}\omega_{,\phi}| \ll 9.45 \times 10^9 \left(\frac{\mathcal{P}_S}{2.441 \times 10^{-9}} \right)^{-1} \left(\frac{r}{0.1} \right)^{-3/2}. \quad (79)$$

Of course, if we allow an appearance of ghost in tensor modes, a situation might be changed drastically. However, it exceeds the scope of this paper.

D. Lyth bound

Here, we comment on the Lyth bound[38]. The statement of this bound is following: If primordial gravitational waves are detected, the variation of inflaton field must exceed a scale on the order of Planck mass. In our model, this bound also holds. From Eq.(16)

$$N = \frac{1}{M_{\text{Pl}}} \int_0^\phi \frac{d\phi}{\sqrt{2\beta}} = \frac{2\sqrt{2}}{M_{\text{Pl}}} \int_0^\phi \frac{d\phi}{\sqrt{r}}, \quad (80)$$

and

$$\delta\phi = \frac{M_{\text{Pl}}}{2} \sqrt{\frac{r}{2}} \delta N. \quad (81)$$

This can be easily understood: Large r corresponds to small $\dot{\phi}$, and this leads to small $\delta\phi$. Note that effect of gravitational waves on the CMB multi pole is relevant in approximately $l \lesssim 100$, which corresponds to $\delta N \simeq 4$. This means that if gravitational waves with tensor-to-scalar ratio r are observed, the field value of inflaton has changed its value approximately $\sqrt{2r}$ during $\delta N \simeq 4$. Hence, from this equation, we can set the lower bound on variation of inflaton field $\Delta\phi$ during whole inflation:

$$\frac{\Delta\phi}{M_{\text{Pl}}} \gtrsim \sqrt{2r} = 0.447 \left(\frac{r}{0.1} \right)^{1/2}. \quad (82)$$

We can see that the Lyth bound holds in our case, while an equation of motion is modified due to the Gauss-Bonnet correction. Therefore, extremely small field inflation, namely $\Delta\phi \ll M_{\text{Pl}}$, cannot produce an observable amount of tensor modes.

IV. INTERESTING FEATURES OF OUR MODEL

In our model, a spectrum of primordial gravitational waves can be blue or scale invariant, and these cases strongly violate the consistency relation $r = -8n_T$. Hence, these (especially, a blue spectrum) are important for confirming our model with future observations. In this section, we use concrete examples to check these interesting situations are consistent with the current WMAP result. We show characteristics of potential and the Gauss-Bonnet coupling function which realize a blue or scale invariant spectrum. We also consider the case in which potential is cancelled out by the Gauss-Bonnet effective potential.

We take e-folding number as $N = 60$ for calculations in examples.

A. Blue spectrum

The most interesting and unique phenomenon in our model might be a blue spectrum of tensor modes. Note that it is impossible to achieve a blue spectrum in a conventional model. For achieving a blue spectrum, $\alpha < 0$ is required. Hence $V_{,\phi} < 0$ is necessary because $\dot{\phi} < 0$. In a case of blue spectrum, a scalar field is climbing up potential, not rolling down. Of course, this blue situation must be over at some time, or inflation lasts forever, because $\dot{H} > 0$ is satisfied in this blue case. A climbing up situation can be understood using Eq.(13), which shows that the coupling function ξ works as effective potential. Hence, if the effective potential ξ is steep enough, ϕ can climb up potential. We show this in FIG.1.

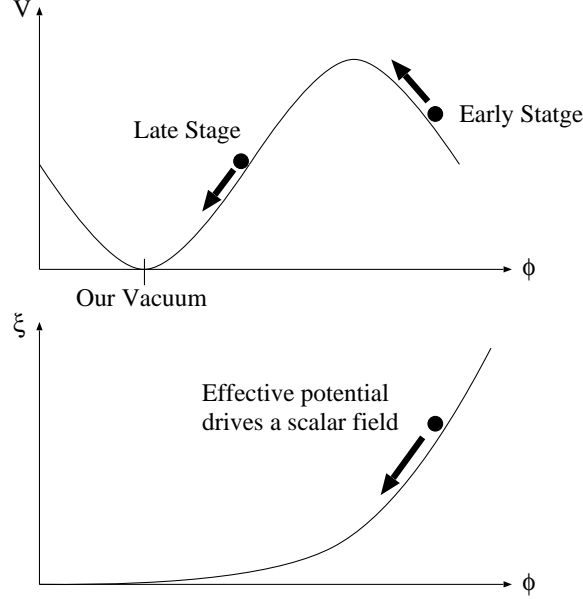


FIG. 1: The configuration of the potential V and the coupling function ξ , which achieve a blue spectrum, is shown. We need a climbing-up situation to realize a blue spectrum. Therefore the following situation is required: At early stage, the effective potential ξ makes ϕ climb up potential and a blue spectrum is realized. At late stage, ϕ rolls down potential as usual.

In a blue spectrum case, $\xi_{,\phi}$ can be calculated by employing Eq.(75) with $\delta > 1$. Hence, there is a necessary condition for a blue spectrum:

$$M_{\text{Pl}}\xi_{,\phi} > \frac{\sqrt{2}}{\pi^2} \frac{1}{\sqrt{r}\mathcal{P}_S} = 1.86 \times 10^8 \left(\frac{\mathcal{P}_S}{2.441 \times 10^{-9}} \right)^{-1} \left(\frac{r}{0.1} \right)^{-1/2}, \quad (83)$$

and combining with Eq.(76)

$$\frac{V_{\xi,\phi}}{M_{\text{Pl}}^3} > \frac{3}{\sqrt{2}} \sqrt{r} = 0.671 \left(\frac{r}{0.1} \right)^{1/2}. \quad (84)$$

Remember $\delta = 1 + 8n_T/r$ and $|n_T| \ll 1$. To observe tensor modes, r cannot take an extremely small value. Hence, δ cannot exceed a value of order unity and $\delta \sim 1$ must hold. In a consistent blue spectrum case, hence, we need the derivative of the Gauss-Bonnet coupling function $\xi_{,\phi}$ on the order of $10^8/M_{\text{Pl}}$ and M_{Pl}^3/V . It is important that both too small and too large a value of $\xi_{,\phi}$ cannot result in a desirable blue spectrum. In other words, if a blue spectrum is detected, $\xi_{,\phi}$ at the CMB scale must be on the order of $10^8/M_{\text{Pl}}$.

In the case that a blue spectrum of tensor modes is confirmed, we can reconstruct the value of $\xi_{,\phi}$, which must be on the order of $10^8/M_{\text{Pl}}$. However, it is unclear whether or not an observationally consistent blue spectrum case can actually be realized; what kind of potential and the Gauss-Bonnet coupling function is likely to realize a blue spectrum. To show these, we use two types of examples of blue spectra. First one is a simple, but analytically solvable model and second one is a somewhat realistic model, which is calculated numerically.

We take the following potential and coupling function:

$$V(\phi) = V_0 \left| \sin \left(\frac{\pi}{2} \frac{\phi}{\phi_0} \right) \right|, \quad \xi_{,\phi}(\phi) = \text{const}. \quad (85)$$

In this case, the e-folding number N can be written analytically:

$$N = \frac{4\phi_0^2}{\pi^2 M_{\text{Pl}}^2} \frac{1}{\sqrt{1+4\theta^2}} \ln \left(\frac{x_1 - x}{x - x_2} \frac{1 - x_2}{x_1 - 1} \right), \quad (86)$$

where

$$x \equiv \cos \left(\frac{\pi \phi}{2 \phi_0} \right), \quad \theta \equiv \frac{V_0 \xi_{,\phi} \phi_0}{3\pi M_{\text{Pl}}^4}, \quad x_1 \equiv \frac{1 + \sqrt{1+4\theta^2}}{2\theta}, \quad x_2 \equiv \frac{1 - \sqrt{1+4\theta^2}}{2\theta} = -\frac{1}{x_1}. \quad (87)$$

Note that x must be in the range $-1 < x_2 < x < 1 < x_1$ and θ represents effect of the Gauss-Bonnet correction. We use x as a variable instead of ϕ and $x < 0$ corresponds to a climbing-up situation and a blue spectrum. To show a realization of blue spectrum, we express x in θ and N :

$$x = \frac{1 + x_1 - (1 + x_2)e^y}{1 - x_2 - (1 - x_1)e^y} = \frac{\sqrt{1+4\theta^2} + 1 + 2\theta + (\sqrt{1+4\theta^2} - 1 - 2\theta)e^y}{\sqrt{1+4\theta^2} - 1 + 2\theta + (\sqrt{1+4\theta^2} + 1 - 2\theta)e^y}, \quad (88)$$

where

$$y \equiv \frac{\pi^2 M_{\text{Pl}}^2}{4\phi_0^2} \sqrt{1+4\theta^2} N = y_0 \sqrt{1+4\theta^2}. \quad (89)$$

Here, we have two parameters in this model, namely θ and y_0 . Let us consider varying θ to realize a blue spectrum in fixed y_0 , which corresponds to fixed ϕ_0 . In the situation that $\theta \gg 1$, Eq.(88) becomes

$$x = \frac{4\theta - e^{2y_0\theta}}{4\theta + e^{2y_0\theta}}. \quad (90)$$

Hence, with sufficiently large θ , $x < 0$ and blue spectrum can be realized for any ϕ_0 value. The condition for a blue spectrum is

$$4(1-q)\theta^2 - 4q\theta + (1-q) < 0, \quad (91)$$

where

$$q \equiv \tanh^2 \left(\frac{y}{2} \right). \quad (92)$$

This inequality is satisfied, only if $1/2 < q < 1$. We define y_b so that $x = 0$ is realized at $y = y_b$. Note that $y < y_b$ and $y > y_b$ correspond to red and blue spectra, respectively. Because $1/2 < q$ is necessary for a blue spectrum, the condition for y_b is

$$y_b > y_c \equiv 2 \tanh^{-1} \frac{1}{\sqrt{2}} = 1.76. \quad (93)$$

Here, we define q_b and θ_b in the same manner as y_b . From Eqs.(89), (91) and (92), we can relate these variables:

$$q_b = \frac{4\theta_b^2 + 1}{(2\theta_b + 1)^2} = \tanh^2 \left(\frac{y_b}{2} \right) = \tanh^2 \left(\frac{y_0 \sqrt{1+4\theta_b}}{2} \right). \quad (94)$$

Note that for $y_0 = y_c/\sqrt{2}$ model, $\theta_b = 1/2$ (and $y_b = y_c$) is the solution for above equations. The scalar spectral index n_S , the tensor spectral index n_T and the tensor-to-scalar ratio r become

$$n_S - 1 = \frac{y_0}{N} \frac{1}{1-x^2} [-2 - x^2 + \theta x(1-x^2)] \quad (95)$$

$$n_T = \frac{y_0}{N} \frac{-x}{1-x^2} [x + \theta(1-x^2)] = \frac{y_0}{N} \frac{\theta x}{1-x^2} (x-x_1)(x-x_2) \quad (96)$$

$$r = \frac{8y_0}{N} \frac{1}{1-x^2} [x + \theta(1-x^2)]^2 = \frac{8y_0}{N} \frac{\theta^2}{1-x^2} (x-x_1)^2 (x-x_2)^2. \quad (97)$$

Let us consider the large θ limit, in which $y \gg y_b$ is satisfied. In this limit, the following equation is realized:

$$x - x_2 = \frac{1 + x_1 - x_2 + x_2^2}{1 - x_2 - (1 - x_1)e^y} \rightarrow 0. \quad (98)$$

Hence, x approaches to x_2 . We define new variable z :

$$z \equiv x + \theta(1 - x^2) = -\theta(x - x_1)(x - x_2) . \quad (99)$$

Because $x \rightarrow x_2$ is realized, $z \rightarrow 0$ holds. Note that $x - x_2$ approaches to zero exponentially as a function of θ , and this leads to $\theta(x - x_2) \rightarrow 0$. Observables become

$$n_S - 1 = -\frac{4y_0}{N}\theta , \quad n_T = \frac{y_0}{N}\theta z , \quad r = \frac{8y_0}{N}\theta z^2 . \quad (100)$$

Note that r becomes small in large θ , because $\theta z \rightarrow 0$. This shows that in any model, this large θ limit results in small r and extremely red n_S . The reason for small r is that $x = x_2$ corresponds to the fixed point, at which potential is cancelled out by effective potential. Hence, $\dot{\phi} = 0$ and $r = 0$ are realized. Since this is not a desirable case, we consider the small θ case, in which $\theta \sim \theta_b$ holds. In this case, $x \sim 0$ is realized, and observables become

$$n_S - 1 = -\frac{2y_0}{N} , \quad n_T = \frac{y_0}{N}(-x\theta_b) , \quad r = \frac{8y_0}{N}\theta_b^2 . \quad (101)$$

Note that θ_b and y_0 are not independent variables, because θ_b is fixed by choosing y_0 . Remember that $\theta_b = 1/2$ is the solution for $y_0 = y_c/\sqrt{2}$ model. Let us substitute these:

$$n_S - 1 = -\frac{\sqrt{2}y_c}{N} = -0.0415 , \quad n_T = \frac{y_c}{2\sqrt{2}N}(-x) = -0.0104x , \quad r = \frac{\sqrt{2}y_c}{N} = 0.0415 . \quad (102)$$

Here, we get good result: n_S and r are consistent with current observations and a blue spectrum of tensor modes is obtained. Therefore, desirable solutions might exist in the vicinity of $\theta \sim 1/2$ and $y_0 \sim y_c/\sqrt{2}$:

$$\phi_0 \sim \frac{2^{1/4}\pi}{2} \sqrt{\frac{N}{y_c}} M_{\text{Pl}} = 10.9 M_{\text{Pl}} , \quad \frac{V_0 \xi_{,\phi}}{M_{\text{Pl}}} \sim \frac{3}{2^{1/4}} \sqrt{\frac{y_c}{N}} = 0.432 . \quad (103)$$

Let us consider the model, in which ϕ_0 is large enough to satisfy $y_0 \ll y_c$. From Eqs.(89) and (93), $y_b = 2y_0\theta_b$ is realized, and r at $x = 0$ becomes

$$r = \frac{4}{N}\theta_b y_b > \frac{4y_c}{N}\theta_b . \quad (104)$$

Because $\theta_b = y_b/2y_0 > y_c/2y_0 \gg 1$, this large field model results in r , which is too large. This is because, in this large field model, inflaton ϕ must roll large field value between the hill-top of potential and the vacuum, within $N = 60$ e-fold. This requires large $\dot{\phi}$, in other words, large r . In addition, from Eq.(101), this large field model also leads to a flat spectrum of scalar modes. In the small field model, which satisfies $y_0 \gg y_c$, the inequality $y \gg 1$ always holds. Hence, as in the above large θ limit, this results in small r and extremely red n_S . Note that larger field models are corresponding to larger values of r , and this is consistent with the consideration in the Lyth bound.

We show θ -trajectories of solutions on a $n_S - r$ plane in FIG.2. We plot the 68% and 95% C.L. contours from the WMAP 7-year result[1]. We choose eight ϕ_0 values surrounding $\phi_0 = 11M_{\text{Pl}}$. Thick dotted and thick solid lines correspond to $0.003 > n_T > 0$ and $n_T > 0.003$ blue spectra. As stated above, models with $\phi_0 \sim 11M_{\text{Pl}}$ have observationally consistent blue regions; large field models correspond to large r and small or no consistent blue spectrum region; small field models have extremely small r ; in large θ limit, r becomes zero and n_S becomes extremely red. It is clear that a consistent blue spectrum model can actually be constructed. To get the value of $\xi_{,\phi}$, we can use Eq.(75). Of course, as mentioned above, $\xi_{,\phi} \sim 10^8/M_{\text{Pl}}$ is realized in a blue region.

Next, we consider a realistic model. To realize a blue spectrum, new-inflation-type potential, as depicted in FIG.1, is required. Therefore, we use forth-order double-well potential and an exponential coupling function:

$$V(\phi) = \rho 10^{-10} M_{\text{Pl}}^4 \left[\frac{(\phi - \phi_0)^2 - \phi_0^2}{\phi_0^2} \right]^2 , \quad \xi(\phi) = s \frac{b}{\rho} \exp(sa\phi/M_{\text{Pl}}) , \quad (105)$$

where $s = \pm 1$, ρ will be fixed by the scalar power spectrum $\mathcal{P}_S = 2.441 \times 10^{-9}[1]$ and $a, b > 0$. We take $\phi = 0$ as our vacuum. We use this exponential coupling, since it appears in many theories, such as a dilatonic case or an one-loop correction from a superstring motivated model[2].

We show b -trajectories on a $n_S - r$ plane in FIG.3. We plot the 68% and 95% C.L. contours from the WMAP 7-year result. We use nine values of a , which varies from 0.01 to 1 with an even logarithmic interval, and three value of ϕ_0 ,

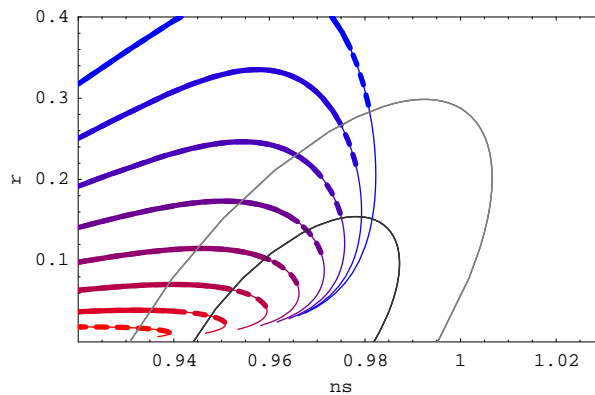


FIG. 2: The trajectories, in which θ is varying, of analytic blue models are shown on a $n_s - r$ plane. Two contours roughly corresponds to the 68% and 95% confidence level of the WMAP 7-year result. We draw eight lines, which are corresponding to $\phi_0 = 9$ (red, bottom) to $16M_{\text{Pl}}$ (blue, top) with an even interval. Thick dotted and thick solid lines denote the blue spectra of $0.003 > n_T > 0$ and $n_T > 0.003$, respectively. Models with $\phi_0 \sim 11M_{\text{Pl}}$ are consistent with observations and realizes blue spectra.

11.1, 15 and $20M_{\text{Pl}}$. We choose ϕ_0 value so that n_s and r values are inside this 68% C.L. contour in the $b \rightarrow 0$ limit. Thick dotted and thick solid lines in FIG.3 denote the blue spectra of $0.003 > n_T > 0$ and $n_T > 0.003$, respectively. We can see it is possible to realize a consistent blue spectrum. The case of $\phi_0 = 15M_{\text{Pl}}$ is appropriate to achieve a consistent blue spectrum. Small ϕ_0 leads to small r and large ϕ_0 leads to a small consistent blue region, and these are essentially consistent with the above analytic case. Due to this exponential coupling, even large field models, namely $\phi_0 = 20M_{\text{Pl}}$ models with $s = -1$, have blue spectrum regions and small field models, namely $\phi_0 = 11.1M_{\text{Pl}}$ models with $s = +1$, have an observable amount of r . This figure shows that an order unity value of a leads to a non-desirable result, which has too small r or no blue region. Therefore $a \ll 1$ is appropriate to obtain a blue spectrum. Moreover, if a is large in $s = -1$ models, it implies the Gauss-Bonnet effect becomes stronger toward the end of inflation. In this case, standard reheating scenarios seem to be broken. Therefore, large a in $s = -1$ models is also not desirable in this sense. Note that with Eq.(75), we can get the value of $\xi_{,\phi}$.

From the above analytic model and this realistic one, we can say that inflationary models with observationally consistent blue spectra can be constructed. Hence, the Gauss-Bonnet coupling function will actually be fixed or constrained with future observations. New-inflation-type potential with the symmetry breaking scale of $\phi_0 \sim 10M_{\text{Pl}}$ and an almost constant form of $\xi_{,\phi}$ might lead to a consistent blue spectrum. Of course, these are not general conditions. However, we can expect many models are also consistent with these conditions. Note that to obtain blue spectrum, $\xi_{,\phi} \sim 10^8/M_{\text{Pl}}$ must be realized in any model at the CMB scale.

B. Scale invariant spectrum

In inflation with a standard gravitational action, a scale invariant spectrum of gravitational waves corresponds to almost purely de Sitter inflation and this requires the tensor-to-scalar ratio r extremely small. However, inflation with the Gauss-Bonnet term behaves differently. Let us consider the case, in which the Gauss-Bonnet term dominate the scalar equation of motion, Eq.(15). The function ζ becomes

$$\zeta = \frac{V^2 \xi_{,\phi}}{6M_{\text{Pl}}^4}, \quad (106)$$

and this requires

$$\frac{\zeta}{V_{,\phi}} = \frac{\beta}{\alpha} \gg 1. \quad (107)$$

In this case, α becomes negligible. Hence

$$n_s - 1 = 2\gamma = 2M_{\text{Pl}}^2 \frac{\zeta_{,\phi}}{V}, \quad n_T = 0, \quad r = 16\beta = 8M_{\text{Pl}}^2 \frac{\zeta^2}{V^2}. \quad (108)$$

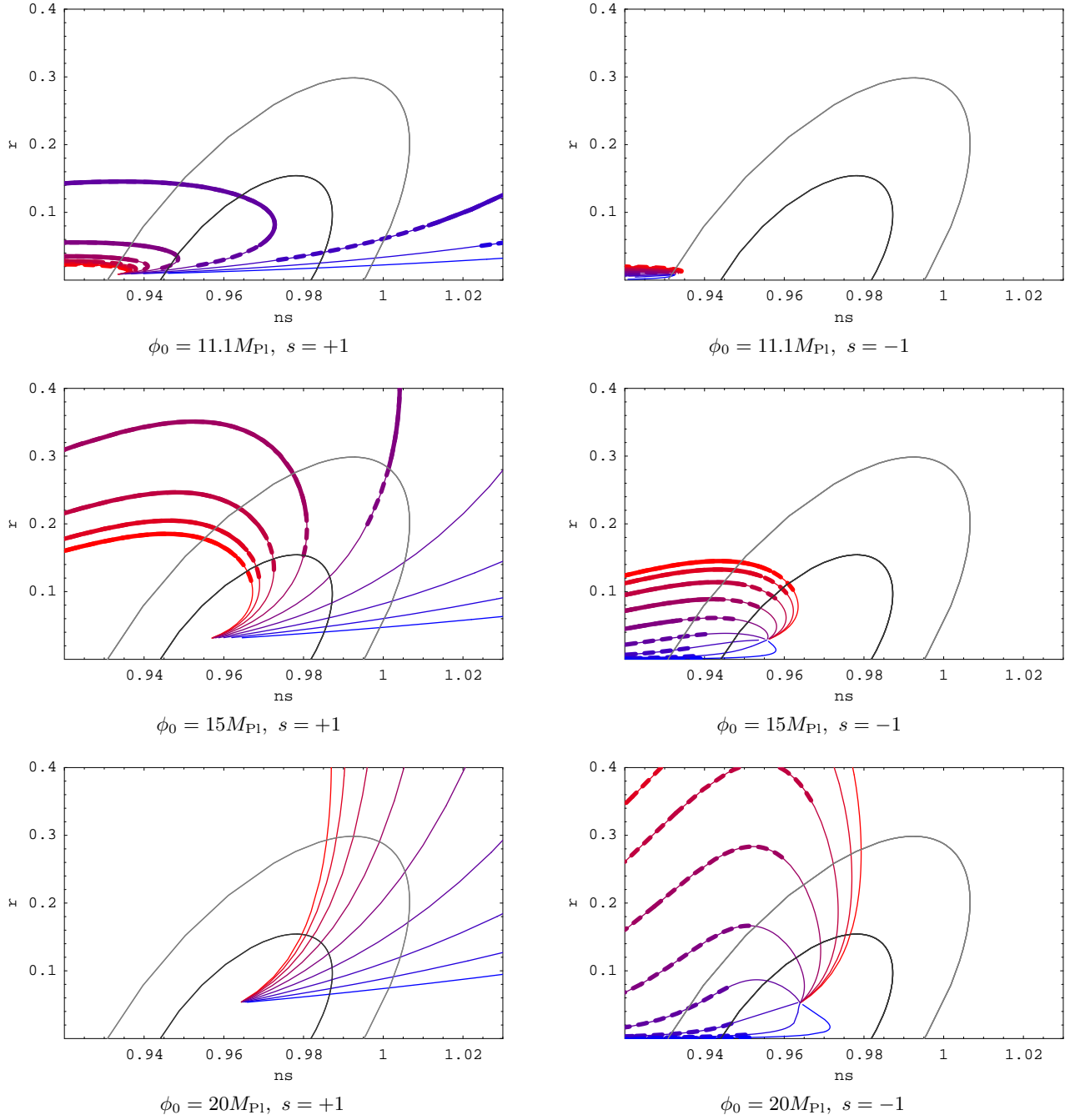


FIG. 3: The trajectories, in which b is varying, of some blue models are shown on a $n_s - r$ plane. In the $b \rightarrow 0$ limit, all trajectories converges to one point. Two contours roughly corresponds to the 68% and 95% confidence level of the WMAP 7-year result. We draw nine lines, which are corresponding to $a = 0.01$ (red, left in left panels and top in right panels) to 1 (blue, right in left panels and bottom in right panels) with an even logarithmic interval. Thick dotted and thick solid lines denote $0.003 > n_T > 0$ and $n_T > 0.003$ blue spectra, respectively. The model with $\phi_0 = 15M_{\text{Pl}}$ is appropriate to achieve blue spectrum. An exponential coupling makes large ϕ_0 ($\phi_0 = 20M_{\text{Pl}}$) model result in a blue spectrum, and small ϕ_0 ($\phi_0 = 11.1M_{\text{Pl}}$) model achieve an observable amount of r .

These equations means that if the Gauss-Bonnet correction dominates this equation of motion, the tensor-to-scalar ratio r can take an observable value although $n_T = 0$ is realized. Because of the consistency relation $r = -8n_T$, this scale invariant spectrum is impossible in a conventional model. Therefore, if scale invariant primordial gravitational waves are detected, it implies existence of the Gauss-Bonnet term in an inflationary theory and $\xi_{,\phi}$ is determined by Eq.(75) with $\delta = 1$:

$$M_{\text{Pl}}\xi_{,\phi} = \frac{\sqrt{2}}{\pi^2} \frac{1}{\sqrt{r}\mathcal{P}_S} = 1.86 \times 10^8 \left(\frac{\mathcal{P}_S}{2.441 \times 10^{-9}} \right)^{-1} \left(\frac{r}{0.1} \right)^{-1/2}, \quad (109)$$

and using Eq.(76)

$$\frac{V\xi_{,\phi}}{M_{\text{Pl}}^3} = \frac{3}{\sqrt{2}}\sqrt{r} = 0.671 \left(\frac{r}{0.1} \right)^{1/2}. \quad (110)$$

As in a blue case, $\xi_{,\phi} \sim 10^8/M_{\text{Pl}}$ and $\xi_{,\phi} \sim M_{\text{Pl}}^3/V$ must be satisfied in this flat spectrum case, too. Both too large and too small a value of $\xi_{,\phi}$ cannot lead to a consistent scale invariant spectrum. From Eqs.(107) and (108), the inequality for r holds:

$$r \gg 8M_{\text{Pl}}^2 \frac{V_{,\phi}^2}{V^2}. \quad (111)$$

This shows that potential must be nearly flat for the tensor-to-scalar ratio r to remain small.

Here, we check whether or not an observationally consistent scale invariant model can be constructed. In this subsection, we also use two types of examples, namely a simple and analytic one and a realistic one. Let us start with an analytic model:

$$V = V_0 \left| \tanh \left(\frac{\phi}{\phi_0} \right) \right|, \quad \xi_{,\phi}(\phi) = \text{const}. \quad (112)$$

The e-folding number N becomes

$$N = \frac{\phi_0^2}{2M_{\text{Pl}}^2} \frac{1}{\theta} \ln(\theta x^2 + 1), \quad (113)$$

where x and θ are defined by

$$x \equiv \sinh \left(\frac{\phi}{\phi_0} \right), \quad \theta \equiv \frac{V_0 \xi_{,\phi} \phi_0}{6M_{\text{Pl}}^4}. \quad (114)$$

We use x instead of ϕ , and x is

$$x^2 = \frac{1}{\theta} \left[\exp \left(\frac{2M_{\text{Pl}}^2}{\phi_0^2} \theta N \right) - 1 \right]. \quad (115)$$

The observables, namely the scalar spectral index n_S , the tensor spectral index n_T and the tensor-to-scalar ratio r become

$$n_S - 1 = \frac{M_{\text{Pl}}^2}{\phi_0^2} \frac{1}{x^2 + 1} \left(-\frac{3}{x^2} - 4 + \theta \right) \quad (116)$$

$$n_T = \frac{M_{\text{Pl}}^2}{\phi_0^2} \frac{1}{x^2 + 1} \left(-\frac{1}{x^2} - \theta \right) \quad (117)$$

$$r = \frac{8M_{\text{Pl}}^2}{\phi_0^2} \frac{1}{x^2 + 1} \left(\frac{1}{x} + \theta x \right)^2. \quad (118)$$

In this model, we also variate θ and fix ϕ_0 .

Let us consider the limit case, in which $\theta \ll \phi_0^2/2M_{\text{Pl}}^2N$ is satisfied, and x becomes

$$x^2 = \frac{2M_{\text{Pl}}^2}{\phi_0^2} N. \quad (119)$$

Hence, observables are

$$n_S - 1 = -\frac{1}{2N} \frac{4x^2 + 3}{x^2 + 1}, \quad n_T = -\frac{1}{2N} \frac{1}{x^2 + 1}, \quad r = \frac{4}{N} \frac{1}{x^2 + 1}. \quad (120)$$

We can see that in this small θ limit, all models give observationally consistent values. Next, we investigate the large θ limit, $\theta \gg \phi_0^2/2M_{\text{Pl}}^2 N$. The variable x takes an exponentially large value in this limit. Hence, observables become

$$n_S - 1 = \frac{M_{\text{Pl}}^2}{\phi_0^2} \frac{\theta}{x^2}, \quad n_T = -\frac{M_{\text{Pl}}^2}{\phi_0^2} \frac{\theta}{x^2}, \quad r = \frac{8M_{\text{Pl}}^2}{\phi_0^2} \theta^2. \quad (121)$$

These show that in this limit, n_S and n_T approach to flat one and r becomes large. Remember that x behaviors exponentially as a function of θ . If this large θ limit is realized in the WMAP consistent region, such as $r < 0.3$, the result which has an observable amount of r and flat n_T is achieved. Here, we consider $\theta = \phi_0^2/2M_{\text{Pl}}^2 N$ case, which is the boundary case between large and small θ . In this case, $1 + x^2\theta = e$ is realized. The observables n_T and r become

$$n_T = -\frac{1}{2N} \frac{e}{e-1} \frac{\theta}{e-1+\theta} = -0.0132 \frac{\theta}{e-1+\theta}, \quad r = \frac{4}{N} \frac{e^2}{e-1} \frac{\theta}{e-1+\theta} = 0.287 \frac{\theta}{e-1+\theta}. \quad (122)$$

If $\theta = \phi_0^2/2M_{\text{Pl}}^2 N > e - 1$ is satisfied, $-n_T > 0.00659$ and $r > 0.143$ hold. This r might be too large to realize that large θ limit in $r < 0.3$. Therefore, to achieve desirable results, $\theta \ll e - 1$ at this $\theta = \phi_0^2/2M_{\text{Pl}}^2 N$ case might be necessary. In other words,

$$\phi_0 \ll \sqrt{2N(e-1)} M_{\text{Pl}} = 14.4 M_{\text{Pl}}. \quad (123)$$

The physical meaning of this condition can be easily understood: Large field model requires large $\dot{\phi}$ and inconsistently large $r (> 0.3)$, to reach a flat potential region within $N = 60$ e-fold. This interpretation is essentially the same as that in the condition for blue spectrum. The difference is that small field model can also achieve large r in this case, because *small* doesn't mean the smallness of the variation of the field value of the inflaton ϕ . It means the smallness of the field value between the vacuum and a flat region of potential. Hence, this is consistent with the Lyth bound. If this condition is satisfied, sufficiently large θ , namely $\theta \gg \phi_0^2/2M_{\text{Pl}}^2 N$, in other words

$$\frac{V_0 \xi_{,\phi}}{M_{\text{Pl}}^3} \gg \frac{3}{N} \frac{\phi_0}{M_{\text{Pl}}}, \quad (124)$$

leads to a consistent flat spectrum.

We show θ -trajectories of solutions on a $n_S - r$ plane in FIG.4. We plot the 68% and 95% C.L. contours from the WMAP 7-year result. We choose five ϕ_0 values, 2, 4, 6, 8 and $10M_{\text{Pl}}$. Thick lines denote the flat region, in which $r/8|n_T| > 100$ is realized. Note that $r = -8n_T$ holds in conventional single field inflation. Therefore large $r/8|n_T|$ value implies a flat spectrum. We can see that small ϕ_0 models, namely $\phi_0 = 2M_{\text{Pl}}$ and $\phi_0 = 4M_{\text{Pl}}$ models, result in WMAP-consistent flat spectra. This is consistent with the criterion at the above calculation, namely $\phi_0 \ll 14.4M_{\text{Pl}}$. As mentioned above, n_S also becomes flat, in a flat tensor region. Note that the smaller field model, namely $\phi_0 = 2M_{\text{Pl}}$ model, has larger consistent scale invariant region. Of course, $\xi_{,\phi}$ can be reconstructed from Eq.(75), and $\xi_{,\phi} \sim 10^8/M_{\text{Pl}}$ must hold in a flat region.

Here, we consider a realistic example of a flat spectrum model. Nearly flat potential results in a Gauss-Bonnet dominating situation. Therefore we take the following potential and coupling function:

$$V(\phi) = \rho 10^{-10} M_{\text{Pl}}^4 \left[1 - \exp\left(-\frac{\phi^2}{\phi_0^2}\right) \right], \quad \xi(\phi) = s \frac{b}{\rho} \exp(sa\phi/M_{\text{Pl}}), \quad (125)$$

where $s = \pm 1$, ρ will be fixed by $\mathcal{P}_S = 2.441 \times 10^{-9}$, and $a, b > 0$. In the $\phi \rightarrow \infty$ limit, this potential becomes extremely flat. We use the same exponential coupling in this example as in previous subsection.

We show b -trajectories on a $n_S - r$ plane in FIG.5. We plot the WMAP 68% and 95% C.L. contours. We use three values of ϕ_0 , 2, 6 and $10M_{\text{Pl}}$, and the same set of a in this case as in the realistic blue spectrum case. Thick lines denote the regions $r/8|n_T| > 100$. As predicted from the previous analytic models, smaller ϕ_0 models has larger regions of flat spectra. Note that $s = -1$ models have larger consistent flat region than that of $s = +1$ models. An order unity value of a leads to extremely small r in both $s = \pm 1$ models, and considering reheating, large a in $s = -1$ models is not desirable. Therefore also in this case, $a \ll 1$ is appropriate. Eq.(75) is valid to get the value of $\xi_{,\phi}$.

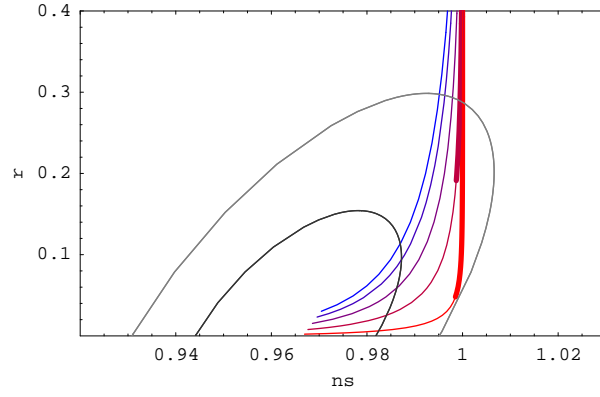


FIG. 4: The trajectories, in which θ is varying, of analytic flat models are shown on a $n_s - r$ plane. Two contours roughly corresponds to the 68% and 95% confidence level of the WMAP 7-year result. We draw five lines, which are corresponding to $\phi_0 = 2$ (red, bottom) to $10M_{\text{Pl}}$ (blue, top) with an even interval. Thick lines denote the regions, which realize $r/|8n_T| > 100$. Small ϕ_0 models, namely $\phi_0 = 2M_{\text{Pl}}$ and $\phi_0 = 4M_{\text{Pl}}$ models, realize observationally consistent flat spectra.

In $s = -1$ models, trajectories approach to some points for each a in large b limit, in FIG.5. This is understood from Eq.(16). In the large b limit of $s = -1$ models, only a large ϕ region contribute to the integration for an e-folding number. Because $V_{,\phi}/V \simeq 0$ in this region, we can omit $V_{,\phi}/V$ term:

$$N = \frac{6M_{\text{Pl}}^2}{V_0} \int_0^\phi \frac{d\phi}{\xi_{,\phi}} = \frac{6M_{\text{Pl}}^3}{aV_0\xi_{,\phi}}. \quad (126)$$

This shows that, in this large b limit, $\xi_{,\phi}$ approaches to $\xi_{,\phi} = 6M_{\text{Pl}}^3/aNV_0$. This also fixes the value of $\xi_{,\phi\phi}$ and all slow-roll parameters. The observables n_s and r become

$$n_s - 1 = \frac{V_0\xi_{,\phi\phi}}{3M_{\text{Pl}}^2} = -\frac{2}{N}, \quad r = \frac{2V_0^2\xi_{,\phi}^2}{9M_{\text{Pl}}^6} = \frac{8}{a^2N^2}. \quad (127)$$

Hence, trajectories approach to some points in large b . This shows that $a \simeq 1$ model leads to very small r because r approaches to $r = 8/N^2 = 0.00222$ at $a = 1$.

From above results, we can say that an observationally consistent flat spectrum can be obtained. Hence, confirming existence of the Gauss-Bonnet term is possible, with observing a scale invariant tensor mode. In the cases we considered, $\phi_0 \ll 10M_{\text{Pl}}$ and nearly constant $\xi_{,\phi}$ might lead to a consistent flat spectrum. Note that ϕ_0 denotes the difference between the filed value of a flat region and the vacuum of potential. We can expect these conditions are also satisfied in many other cases. To realize a flat spectrum, $\xi_{,\phi} \sim 10^8/M_{\text{Pl}}$ is necessary in any model.

C. Inflation with steep potential

As mentioned in the end of section II, if we take $\xi = 6M_{\text{Pl}}^4/V$, potential is cancelled out by the Gauss-Bonnet effective potential. Considering this fact, let us take ξ as follows:

$$\xi = (1 - \kappa) \frac{6M_{\text{Pl}}^4}{V}, \quad (128)$$

where κ is a constant and we assume $|\kappa| \ll 1$. The function ζ becomes

$$\zeta = V_{,\phi} - (1 - \kappa)V_{,\phi} = \kappa V_{,\phi}. \quad (129)$$

Eq.(15) becomes

$$\frac{\dot{\phi}}{M_{\text{Pl}}H} = -\kappa M_{\text{Pl}} \frac{V_{,\phi}}{V}. \quad (130)$$

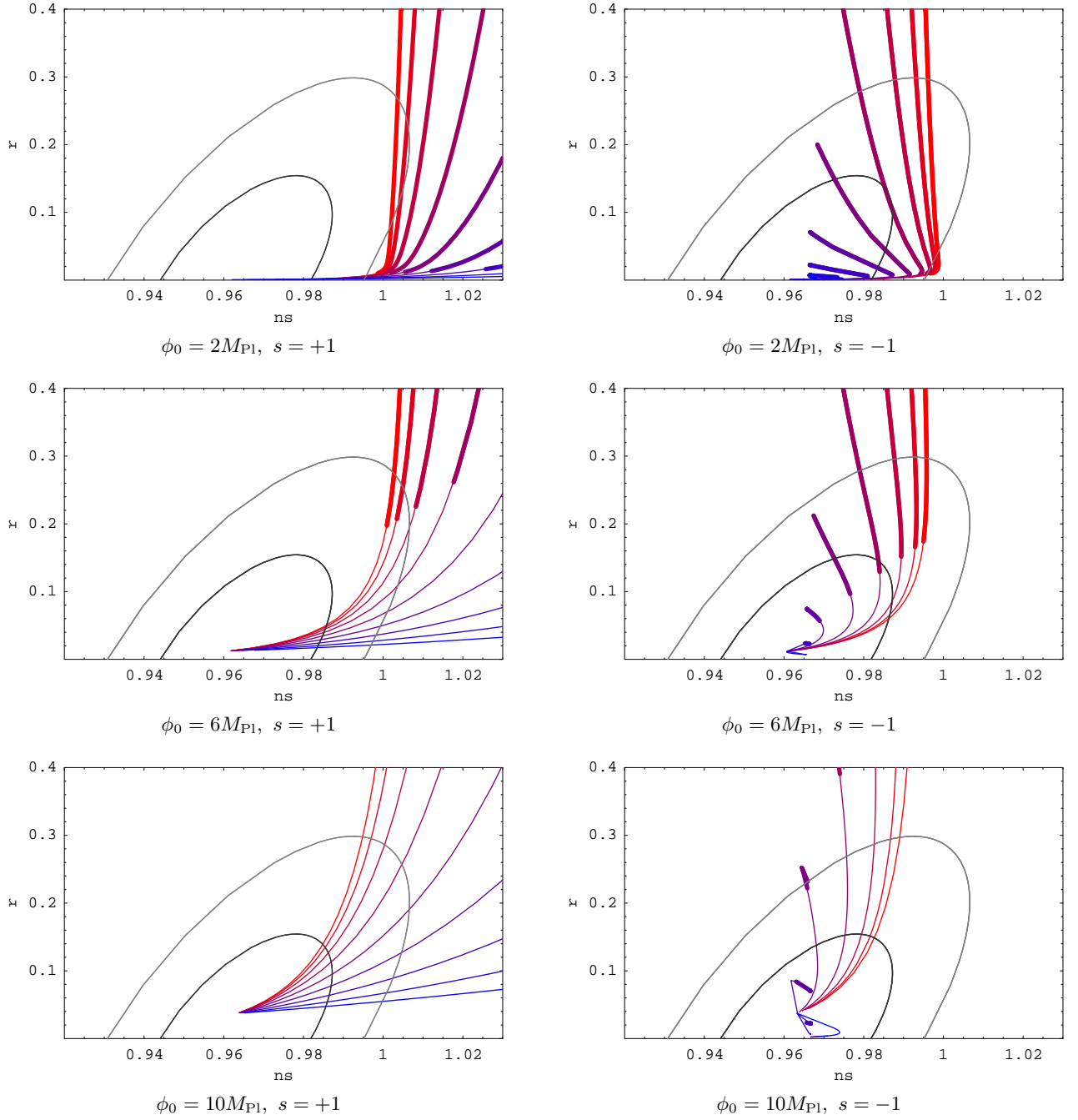


FIG. 5: The trajectories, in which b is varying, of some flat models is shown on a $n_s - r$ plane. In the $b \rightarrow 0$ limit, all trajectories converges to one point. Two contours roughly corresponds to the 68% and 95% confidence level of the WMAP 7-year result. We draw nine lines, which are corresponding to $a = 0.01$ (red, left in left panels and right in right panels) to 1 (blue, right in left panels and left in right panels) with an even logarithmic interval. In this case, tensor spectrum is always red. Thick lines denote the regions of flat spectra, $r/8|n_T| > 100$. This figure shows that small ϕ_0 leads to a flat spectrum. Note that in $s = -1$ models, trajectories approach to some points, in large b limit.

Hence if $\kappa < 0$ is realized, a scalar field always rolls up potential toward a hill-top. This is not a desirable situation. Therefore we take $0 < \kappa \ll 1$. Slow-roll parameters becomes

$$\alpha = \kappa \frac{M_{\text{Pl}}^2}{2} \frac{V_{,\phi}^2}{V^2}, \quad \beta = \kappa^2 \frac{M_{\text{Pl}}^2}{2} \frac{V_{,\phi}^2}{V^2} \simeq 0, \quad \gamma = \kappa M_{\text{Pl}}^2 \frac{V_{,\phi\phi}}{V}, \quad (131)$$

where we used $\kappa \ll 1$. In this case, β becomes negligible. Note if the Gauss-Bonnet term is dominating, α becomes negligible. In this case, the observables n_S , n_T and r are

$$n_S - 1 = -6\alpha + 2\gamma, \quad n_T = -2\alpha, \quad r = 0. \quad (132)$$

Because the tensor-to-scalar ratio r is zero, the value of the spectral index n_T is meaningless. Therefore observationally speaking, this situation is not interesting. However, because $\kappa \ll 1$, three slow-roll conditions are automatically satisfied. Hence, even if we use extremely steep potential, inflation can be achieved.

V. CONCLUSION

In this paper, we studied slow-roll inflation with the Gauss-Bonnet and Chern-Simons corrections. We defined three slow-roll parameters, while we used five parameters in the previous paper[35]. We derived expressions for the scalar spectral index n_S , the tensor spectral index n_T , the tensor-to-scalar ratio r and the circular polarization ratio Π by using these parameters. We showed that in our model, the consistency relation $r = -8n_T$ is not automatically satisfied. If this violation is observationally confirmed, we can determine the derivative of the Gauss-Bonnet coupling function $\xi_{,\phi}$ at the CMB scale. In our model, even both blue and scale invariant spectra of gravitational waves can be realized. Because blue and scale invariant mean $n_T > 0$ and $|8n_T|/r \ll 1$, respectively, these cases violate this consistency relation strongly. Therefore these are the key for confirming our model in future observations. We showed that if either a blue spectrum or a scale invariant one is observed, it supports existence of the Gauss-Bonnet coupling function of $\xi_{,\phi} \sim 10^8/M_{\text{Pl}}$ at the CMB scale. We checked whether or not these blue and scale invariant spectra are consistent with current observations. For this purpose, we used concrete examples. We showed that new-inflation-type potential with $10M_{\text{Pl}}$ symmetry breaking scale and potential with flat region in $\phi \gtrsim 10M_{\text{Pl}}$ might result in observationally consistent blue and scale invariant spectra, respectively. An almost linear form of the Gauss-Bonnet coupling function is appropriate in both cases. These tell us that the detection of a blue or scale invariant spectrum of tensor modes can be actually expected with future observations. We also showed that if circular polarization of gravitational waves is detected, the derivative of the Chern-Simons coupling $\omega_{,\phi}$ must be on the order of $10^8/M_{\text{Pl}}$. Thus, we can say that existence of gravitational higher coupling terms in a inflationary model will be confirmed, or at least constrained, with future experiments.

These higher curvature terms are expected to appear in non-Gaussian part of perturbations. Therefore, calculating non-Gaussianity in our model is important future work.

We would like to thank Jiro Soda for his very useful comments.

-
- [1] E. Komatsu *et al.*, arXiv:1001.4538[astro-ph.CO].
 - [2] I. Antoniadis, J. Rizos and K. Tamvakis, Nucl. Phys. B **415**, 497 (1994) [arXiv:hep-th/9305025].
 - [3] S. Kawai and J. Soda, Phys. Rev. D **59**, 063506 (1999) [arXiv:gr-qc/9807060].
 - [4] S. Kawai and J. Soda, arXiv:gr-qc/9906046.
 - [5] S. Kawai and J. Soda, Phys. Lett. B **460**, 41 (1999) [arXiv:gr-qc/9903017].
 - [6] J. c. Hwang and H. Noh, Phys. Rev. D **61**, 043511 (2000) [arXiv:astro-ph/9909480].
 - [7] C. Cartier, J. c. Hwang and E. J. Copeland, Phys. Rev. D **64**, 103504 (2001) [arXiv:astro-ph/0106197].
 - [8] S. Kawai, M. a. Sakagami and J. Soda, Phys. Lett. B **437**, 284 (1998) [arXiv:gr-qc/9802033].
 - [9] J. Soda, M. a. Sakagami and S. Kawai, arXiv:gr-qc/9807056.
 - [10] S. Kawai, M. a. Sakagami and J. Soda, arXiv:gr-qc/9901065.
 - [11] M. Gasperini, Phys. Rev. D **56**, 4815 (1997) [arXiv:gr-qc/9704045].
 - [12] C. Cartier, E. J. Copeland and M. Gasperini, Nucl. Phys. B **607**, 406 (2001) [arXiv:gr-qc/0101019].

- [13] B. M. Leith and I. P. Neupane, JCAP **0705**, 019 (2007) [arXiv:hep-th/0702002].
- [14] Z. K. Guo, N. Ohta and S. Tsujikawa, Phys. Rev. D **75**, 023520 (2007), [arXiv:hep-th/0610336].
- [15] S. E. Vazquez, Phys. Rev. D **79**, 043520 (2009), arXiv:0806.0603 [hep-th].
- [16] S. Nojiri, S. D. Odintsov and M. Sasaki, Phys. Rev. D **71**, 123509 (2005) [arXiv:hep-th/0504052].
- [17] I. P. Neupane and B. M. N. Carter, JCAP **0606**, 004 (2006) [hep-th/0512262].
- [18] K. T. Koivisto and D. F. Mota, Phys. Lett. B **644**, 104 (2007) [arXiv:astro-ph/0606078].
- [19] K. T. Koivisto and D. F. Mota, Phys. Rev. D **75**, 023518 (2007) [arXiv:hep-ph/0609115].
- [20] I. P. Neupane, arXiv:0711.3234[hep-th].
- [21] I. P. Neupane, Class. Quant. Grav. **23**, 7493 (2006) [hep-th/0602097].
- [22] A. D. Felice and S. Tsujikawa, Phys. Lett. B **675**, 1 (2009), arXiv:0810.5712[hep-th].
- [23] A. D. Felice and S. Tsujikawa, Phys. Rev. D **80**, 063516 (2009), arXiv:0907.1830[hep-th].
- [24] A. D. Felice, D. F. Mota and S. Tsujikawa, Phys. Rev. D **81**, 023532 (2010), arXiv:0911.1811[gr-qc].
- [25] A. D. Felice and S. Tsujikawa, Living Rev. Rel. **13**, 3 (2010), arXiv:1002.4928[gr-qc].
- [26] A. Lue, L. M. Wang and M. Kamionkowski, Phys. Rev. Lett. **83**, 1506 (1999) [arXiv:astro-ph/9812088].
- [27] K. Choi, J. c. Hwang and K. W. Hwang, Phys. Rev. D **61**, 084026 (2000) [arXiv:hep-ph/9907244].
- [28] S. Alexander and J. Martin, Phys. Rev. D **71**, 063526 (2005) [arXiv:hep-th/0410230].
- [29] D. H. Lyth, C. Quimbay and Y. Rodriguez, JHEP **0503**, 016 (2005) [arXiv:hep-th/0501153].
- [30] M. Satoh, S. Kanno and J. Soda, Phys. Rev. D **77**, 023526 (2008), arXiv:0706.3585[astro-ph].
- [31] S. Saito, K. Ichiki and A. Taruya, JCAP **0709**, 002 (2007), arXiv:0705.3701 [astro-ph].
- [32] N. Seto, Phys. Rev. Lett. **97**, 151101 (2006) [arXiv:astro-ph/0609504].
- [33] N. Seto and A. Taruya, Phys. Rev. Lett. **99**, 121101 (2007), arXiv:0707.0535 [astro-ph].
- [34] S. Weinberg, Phys. Rev. D **77**, 123541 (2008), arXiv:0804.4291 [hep-th].
- [35] M. Satoh and J. Soda, JCAP **0809**, 019 (2008), arXiv:0806.4594[astro-ph].
- [36] Z. K. Guo and D. J. Schwarz, Phys. Rev. D **81**, 123520 (2010), arXiv:1001.1897[hep-th].
- [37] V. F. Mukhanov and A. Vikman, JCAP **0602**, 004 (2006) [arXiv:astro-ph/0512066].
- [38] D. H. Lyth, Phys. Rev. Lett. **78**, 1861 (1997) [arXiv:hep-ph/9606387].